Department of Atmospheric & Space Sciences

University of Pune

M.Sc Project Report

On
"Photo-polarimetric variations of T Tauri stars"

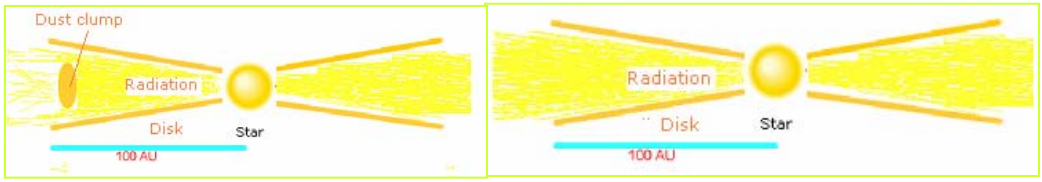

By:	Guide: Prof. A. N. Ramaprakash,
Amit Shukla	IUCAA, Pune, India.
03ss19 Department of Atmospheric & Space Sciences, University of Pune, Pune	Co-Guide: Prof.T.H.Date, DASS, University of Pune, Pune, India.

Contents:

Abstract

The main objective of this research is the study of photo-polarimetric variation of T Tauri star and tries to understand UX Ori **(UXOR)** phenomenon of T Tauri stars. T Tauri stars (TTS) are newly born, roughly solar mass stars that have only recently emerged from their parent molecular cloud cores to become optically visible. T Tauri stars show increased polarization when the optical light of the star is faint this phenomenon is know as UXOR phenomenon To understand this phenomenon we were made polarimetric observation in R band by using an imaging polarimeter (IMPOL) mounted on VBT (Vainu Bappu telescope) at VBO (Vainu Bappu observatory). This report discusses about polarized radiation, origin of polarization in astronomical sources & its mechanisms especially in T Tauri stars.

1. Introduction

The formation and evolution of a star and its stellar system is an open problem of astrophysics in the present scenario. Scientists have suggested that accretion process from a proto-planetary dust disk into the central star plays a very crucial role in the formation of stellar system. These proto-planetary disks contain some inhomogeneities in its structure. To understand the structure and inhomogeneities present in the dust disk like dust clump and hotspots we have chosen a problem of photoplarimetric variation in classical type T Tauri (CTTS) for our studies.

Polarization arises in astronomical sources due to asymmetry or anisotropy. Such asymmetry may be within the source itself or in the medium between the source and the observer, or both. The most common asymmetries are magnetic field and geometric asymmetries like non-spherical cloud, disks, jets or blobs. A lot of dust is present around the pre-main-sequence (PMS) stars in the form of disk or circumstellar envelops of newborn stars and this is one of the causes of polarization of light from PMS.PMS are very young objects of for ages less than about 10^6 year. T Tauri star is a classical example of PMS.

The source may be intrinsically polarized as in the case of beamed emission in strong magnetic fields, synchrotron emission; or the radiation may be polarized by scattering from clouds, jets, disks or blobs. The polarization properties can also be modified by the intervening interstellar medium. Thus measurements of the polarization provide unique information on the nature of astronomical sources.

The T Tauri stars are the most well known class of pre-main sequence stars. They are low- to intermediate-mass stars with ages of typically a few million years. At this stage in their evolution, the newly collapsed stars have become optically visible but are still surrounded by gas and dust from their formation, typically in a disk. The first measurement of polarization, in T Tauri stars (TTS), was made by Vardanyan (1964) and Serqowiski (1969). Since then polarimetric observations of number of a TTS have shown that variability in both the degree of polarization and position angle is common property of this class of object. But the origin of observed

variability of the linear polarization is not well known. Change in geometry of scattering environment, caused by inhomogeneities in a circumstellar disk or by orbiting blobs and variable illumination of the circumstellar material by the central star, are among different potential possibilities for polarization variation that have been proposed.

To further understand this phenomenon we have made simultaneous photo-polarimetric observations in **R** band by using IMPOL (Imaging polarimeter) at V.B.T (Vainu Bappu telescope) Kavalur. We have observed four T Tauri stars of different properties the names of these stars are given as follows Su Aur, Bf Ori, Ux Ori and Co ori. This report contains nine chapters. From the second chapter and onwards I have discussed about polarization, calculation of polarization, T Tauri stars, instruments which are used for observation and the results.

Second chapter contains discussion about polarization. In this chapter I have given brief information about Stoke parameters and type of polarizations. In the chapter three I have given brief information about the instruments, which are used for observation. The forth and fifth chapter contains polarization in astronomy and a brief discussion about T Tauri star and its mechanism of polarization. The chapters six, seven and eight contain the discussion about calculation of polarization, data collection and data reduction respectively. In the chapter nine I have shown the results that are based on calculation of polarization. Conclusion is also discussed in this chapter.

2. Polarization

Ordinary white light is made up of wave that fluctuates at all possible angle. Light is considered to be linearly polarized when it contains waves that only fluctuate in specific plane and polarizer is a device, which allows only one mode of such oscillation to pass through it. We know that an electromagnetic wave is a transverse wave and the directions of electric field and magnetic field is mutually perpendicular to each other and to its direction of propagation. We can represent quasi-monochromatic light in terms of two orthogonal linear polarization components by using the complex notation,

$$E_x = E_{x_o}(t)e^{i(\phi+\phi_x(t))} \quad \& \quad E_y = E_{y_o}(t)e^{i(\phi+\phi_y(t))} \qquad \text{---------(2.1)}$$

where, the propagation constant, $\phi = \omega\, t + kz$.

In this chapter I have discussed about type of polarization and Stoke's parameters**.**

2.1 Polarization ellipse

We can define a polarization ellipse as from the help of eq^n(2.1)

$$\left(\frac{E_x}{E_{x_o}}\right)^2 + \left(\frac{E_y}{E_{y_o}}\right)^2 - \frac{2E_xE_y\cos(\phi_x-\phi_y)}{E_{x_o}E_{y_o}} = \sin^2(\phi_x-\phi_y) \qquad \text{--------- (A)}$$

2.2 Linear polarization

Linear polarization is a special case of polarized light. If two orthogonal components of the light wave, one polarized in x-y plane and other in y-z plane reach their maximum and minimum at same time (they are in phase) i.e.

$$\phi_x - \phi_y = 0^o$$

the resultant light wave is linearly polarized at 45 ^{o}.

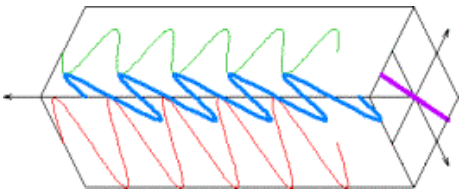

Figure (2.1): Representation of linear polarization

2.3 Circular polarization

If the two orthogonal components are equal in magnitudes ($E_{x_o} = E_{y_o}$) but they are 90^o out of phase i.e.

$$\phi_x - \phi_y = 90^o$$

then resultant light wave is circularly polarized.

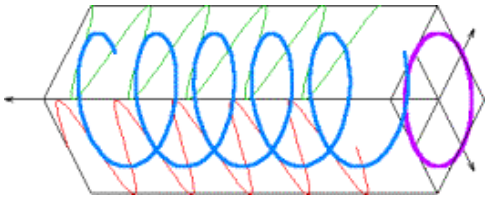

Figure (2.2): Representation of circular polarization

2.4 Elliptical polarization

The most general case is when the phase difference is an arbitrary angle and magnitudes of components are not equal. This is called elliptical polarization because the electric field vector traces out an ellipse.

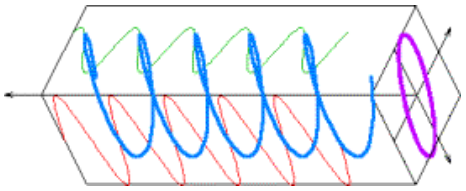

Figure (2.3): Representation of circular polarization

2.5. Stokes parameters

The Stokes vector provides a matrix formalism to represent fully, partially polarized as well as unpolarized light. The four element of the vector, which is known as Stokes parameters are defined in terms of electric field vector as

$$S = \begin{bmatrix} I \\ Q \\ U \\ V \end{bmatrix} = \begin{bmatrix} < E_x E_x^* > + < E_y E_y^* > \\ < E_x E_x^* > - < E_y E_y^* > \\ < E_x E_y^* > + < E_y E_x^* > \\ i(< E_x E_y^* > - < E_y E_x^* >) \end{bmatrix} \qquad \text{-------- (2.2)}$$

where the angular brackets < > represent averaging over time scales in which the measurements are made. These time scales are usually much longer than that corresponding to $1/\omega$.

The first Stokes parameter **I** is the total intensity of the light, the second one **Q** is the difference in intensities between two orthogonal linear polarization components measured in the reference coordinate system. The third parameter **U** is similar to Q but measured in a coordinate system rotated by 45^o with respect to the first one. Q and U are related to the fractional linear polarization **p** and its position angle θ by the relations

$$Q = Ip\cos(2\theta) \qquad \& \qquad U = Ip\sin(2\theta)\,. \qquad \text{-------(2.3)}$$

V is the difference in intensities between the right and left circularly polarized components in the light and is called the circularity parameter. On substituting Eq^n (2.1) into Eq^n (2.2) it reduces to

$$S = \begin{bmatrix} I \\ Q \\ U \\ V \end{bmatrix} = \begin{bmatrix} < E_{x_o}^2 + E_{y_o}^2 > \\ < E_{x_o}^2 - E_{y_o}^2 > \\ < 2E_{x_o}E_{y_o}^* \cos(\phi_x - \phi_y) > \\ (< 2E_{x_o}E_{y_o}^* \sin(\phi_x - \phi_y) > \end{bmatrix} \qquad \text{..... (2.4)}$$

The radiated electric field due to an accelerating charge in polar coordinates can be given as

$$E_\theta = \left(\frac{q}{c^2 R}\right)[\ddot{x}\cos\theta - \ddot{z}\sin\theta] \qquad \text{and} \qquad E_\phi = \left(\frac{q}{c^2 R}\right)\ddot{y} \qquad \text{-------(2.5)}$$

so now, we can also write the Stoke's vector in the polar coordinate system as

$$S = \begin{bmatrix} I \\ Q \\ U \\ V \end{bmatrix} = \begin{bmatrix} < E_\phi E_\phi^* > + < E_\theta E_\theta^* > \\ < E_\phi E_\phi^* > - < E_\theta E_\theta^* > \\ < E_\phi E_\theta^* > + < E_\theta E_\phi^* > \\ i(< E_\phi E_\theta^* > - < E_\theta E_\phi^* >) \end{bmatrix} \qquad \text{----------(2.6)}$$

- Only three of the four Stokes parameters are independent for fully polarized light since

$$I^2 = Q^2 + U^2 + V^2$$

- Unpolarized light has

  Q = U = V = 0

- And for partially polarized light

$$I^2 > Q^2 + U^2 + V^2$$

- For unit intensity (I=1), linearly polarized light has

  V = 0 Q=cos 2θ U=sin 2θ

  So that

  $Q^2 + U^2 = 1$

  The degree of the linear polarization is defined by

$$\frac{\sqrt{Q^2 + U^2}}{I} \leq 1$$

- Circular polarization implies

  Q = U= 0 V=±1

The sign determine the sense of rotation of the electric vector .The degree of circular polarization is

$$-1 \leq \frac{V}{I} \leq 1$$

3. Instruments

3.1 VAINU BAPPU TELESCOPE

The Vainu Bappu telescope (VBT) at Vainu Bappu observatory (VBO) is the largest telescope in Asia. It is an equatorially mounted telescope with a primary mirror of diameter 2.34 m.

Technical Details

- Primary mirror diameter: 2.34 m
- Prime focus: f/3.25 with a scale of 27". 1/mm
- Cassegrain focus: f/13 with a scale of 6".8/mm
- Guiding: remote, manual guiding

3.2. IMPOL (An Imaging polarimeter)

The principle of the instrument (Sen & Tandon 1994) is based on a combination of ideas suggested by Ohman (1939) and Appenzeller (1967).

As shown in fig (3.2) this instrument mainly contains three optical part as follows half wave plate, Wollaston prism & camera lens.

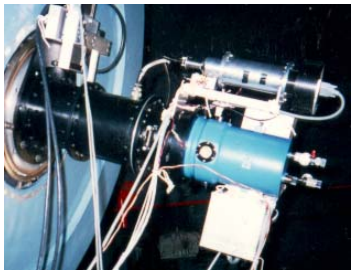

Figure (3.1) IMPOL

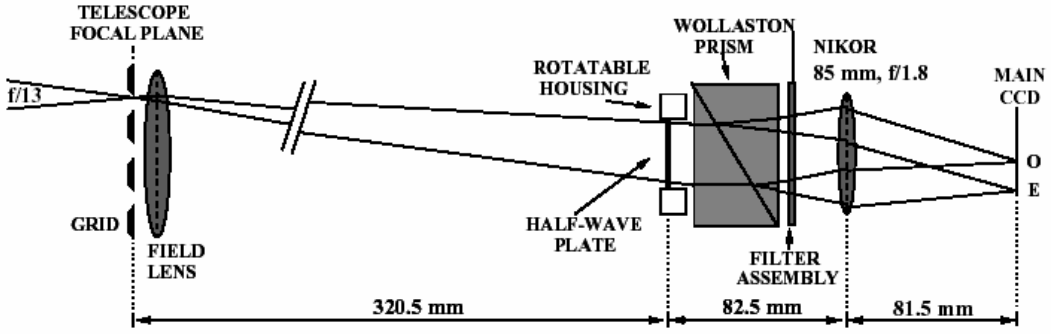

Figure (3.2) Optical bench of IMPOL

The camera lens acts as a focal reducer that reimages the telescope focal plane on the surface of a CCD, with a reduction factor of about 3.8. A **Wollaston prism** is placed just before the camera lens in this assembly, it splits the incident ray into two orthogonal polarized components parallel & perpendicular to the axis of the Wollaston prism, called ordinary (I_o) and extraordinary ray (I_e). These rays travel in slightly different directions.

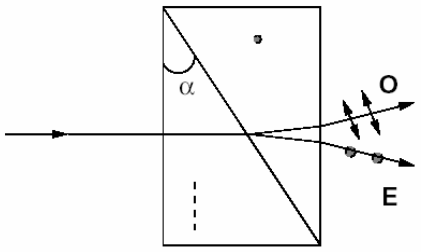

Figure (3.3) Wollaston prism

A Wollaston prism **(figure 3.3)** is made by the two right angle prisms those are glued back to back. The optic axes of the two prisms are perpendicular to the incident ray as well as to each other. The normally incident ray is not deviated as it enters the first prism. However, at the interface, the ordinary ray in the first prism (with vibrations orthogonal to the optic axis) becomes an extraordinary ray in the second one and since $\mathbf{n_e}$ is less than $\mathbf{n_o}$ (for positive crystals) it deviates away from the normal here $\mathbf{n_e}$ and $\mathbf{n_o}$ are the refractive indexes of two orthogonal components. On the other hand, the extraordinary ray (with vibrations along the optic axis) in the first prism becomes an ordinary ray in the second one and refracts towards the normal at the interface. Both of these rays deviate away from the normal as they emerge from the surface of the Wollaston prism and hence their separation increases further. The total separation between the beams depends on the two refractive indices, n_e and n_o as well as the angle α.

When ordinary & extraordinary rays travel in birefringent material they acquire a phase difference because of the different velocities of ordinary and extraordinary rays in birefringent material .A half-wave plate is a retardation plate whose thickness is such that the path difference between the extraordinary and ordinary rays correspond to $\lambda/2$., The equation which govern half wave plate is

$$(n_o - n_e) \times t = \frac{\lambda}{2}$$

3.3. The Acquisition and Guidance (A & G) System

Telescopes have a system with which it tracks a target in the sky. The accuracy of the tracking and guiding depends upon the technology, which is used in the telescope for tracking. The earliest A&G systems used a smaller guide telescope that has wider field of view than main telescope. For pointing and guiding it ensures that the telescope tracks the movement of the object across the sky with sufficient accuracy so that long exposures may be taken. Tracking also may be done using the image in the guide telescope. But the main limitation of such a scheme is its limited sensitivity due to the relatively smaller size of the guide telescope.

For a polarimetric observation we need an accuracy of 2-3 arcsec assuming that the telescope has his own pointing accuracy of about an arc minute. At the time of observation, targets trails due to limitation of the tracking of telescope. So to avoid this problem, in IMPOL an A&G system is introduced, which help the telescope for tracking and pointing targets in the sky. And using this system we can track a target for a long time.

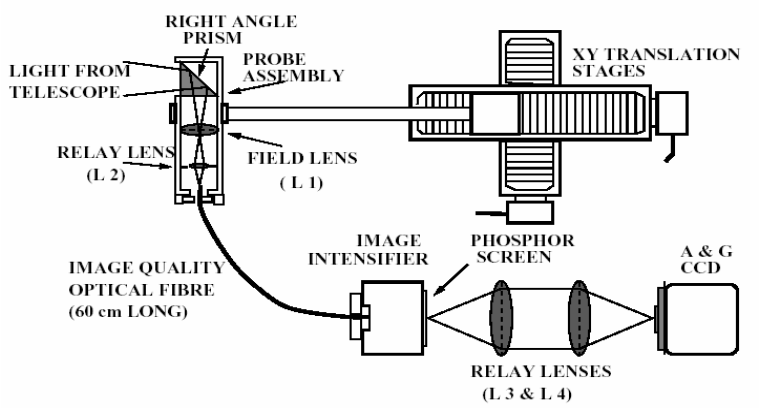

Figure (3.4) IMPOL A&G system

The IMPOL A&G system contains mainly four parts as shown in figure. The positioning of the probe assembly which contains a right angle prism, a field lens (L1) and a relay lens (L2) is set to like this that the prism turn the light coming form the telescope and brings the focus close to field lens. The relay lens is at the focal plane of the field lens and it reimages the telescope focal plane onto the tip of

the optical fibre. And the other end of the optical fibre coupled to the photocathode of the image intensifier. After the image intensifier two-relay lens are placed they reimages phosphor screen on the surface of the CCD of A&G.

Along with every polarimetric observation target, at least one guide star is identified, the image of which is formed by the telescope within the scan area that can be covered by the probe, The right ascension and declination coordinates of the centre of the observation target as well as the guide star is given to the control computer, which in turn calculates the corresponding offset needed for the probe, relative to the center of the main field, and positions it accordingly. In order to acquire the target in the main field, it is sufficient to ensure that the guide star is centred in the field of view of the A&G system. Once the target is acquired, tracking is activated, which involves taking an exposure of the guide field, determining the shift in the centroid of the guide star image with respect to the centre of the field and generating signals which correct the telescope pointing so as to bring the guide star image to the centre of the field. The control computer repeats the above sequence of operations every three seconds or so, until the tracking is stopped.

4. Polarization in Astronomy

4.1 ASTRONOMICAL POLARIMETRIC SOURCES

Magnetic fields are very important phenomenon in this universe; polarimetry is the most basic & direct tool to understand the magnetic fields of astronomical sources because magnetic fields play a crucial role in the polarization of light. The range of the astronomical magnetic fields is quite large. It varies form **10 μG** to interstellar space to **10^{13} G** for pulsars **(Tinbergen 1996).**

The Zeeman Effect is detected in optical spectrum of some magnetic White Dwarfs due to their strong magnetic fields. This magnetic field distorts the spectrum and produces linear & circular polarization. The mechanism of the polarization is cyclotron emission from magnetic fields.

The magnetic field of pulsars can be studied by measuring the variation of polarization in radio pulses, mostly linear & circular.

At radio wave lengths polarization has been detected from supernova remnants, quasars and active galaxies. This polarization is almost linear and arises from synchrotron radiation. Galactic magnetic field is also detected by the same method.

4.2 Synchrotron Radiation

The electromagnetic radiation emitted by relativistic charged particle circulating in a uniform magnetic field under the effect of Lorenz force,

$$\mathbf{F} = q\,(\mathbf{v} \times \mathbf{B})$$

is called Synchrotron radiation**.** An electron of energy of 10^{12} eV may emit synchrotron radiation when it circulates or spirals in a magnetic field of 10^{-3} Gauss.

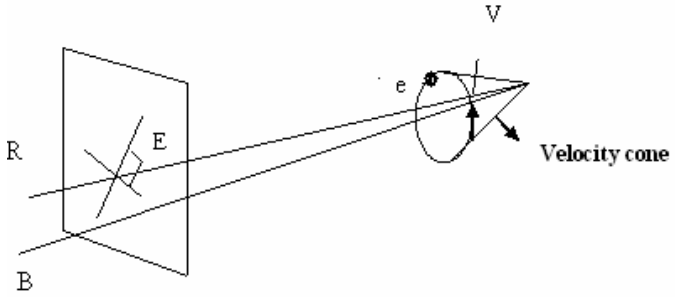

Figure (4.1) Geometry of Synchrotron Radiation

This radiation is highly beamed in a narrow cone of angle **1/γ** in the direction of velocity vector. The axis of the cone is parallel to the magnetic field vector.

Where γ is

$$\gamma = \frac{1}{\sqrt{1-\frac{v^2}{c^2}}}$$

In the case of relativistic electron, however, a significant amount of radiation is only observed if the trajectory of the electron lies within an angle **1/γ** of the line of sight **(M.S.Longair 1992)** and the observed radiation is linearly polarized parallel to the direction **(v x B)** and lying in the plane perpendicular to the wave vector **k** (in plane of motion).

But if the observed radiation is not lying in the cone of angle $1/\gamma$ then there is also a component of polarization in the direction of magnetic field and radiation by a single electron is elliptically polarized due to different time dependence with in each pulse compared to the perpendicular component.

The total net polarization can de determined by integrating over all particles, which contribute to intensity. When the electrons are highly relativistic the component of elliptical polarization parallel to magnetic field cancels out.

The fractional polarization of synchrotron radiation can be as high as 72% and linear.

4.3 Scattering Geometry as a source of Polarization

The dust particles present in an interstellar medium scatter and absorb unpolarized radiation. The scattered light reaching the observer is partially polarized. The scattering properties depend upon the shape, structure and composition of the dust. The theory of scattering has been developed for well-defined particle shapes like spheres, cylinders spheroids, and so on.

The scattering properties of dust grain depend on size parameter $2\pi s/\lambda$, where s is a size of particle and λ is wavelength of incident radiation. In addition, it depends on the property of the grain usually specified by the complex refractive index

$$m(\lambda) = n(\lambda) - ik(\lambda) \qquad \text{----------(4.1)}$$

Where n (λ) and k (λ) are the refractive and absorptive indices respectively **(Pavan Chakraborty 2002)**

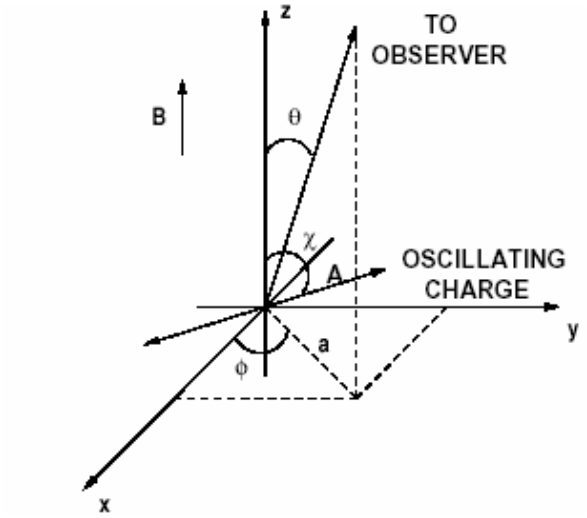

Figure (4.2): Dipole radiation

When an electromagnetic radiation passes through a cloud of air or dust, the electrons of the molecules start to oscillate and this system re-radiates in various direction due to acceleration of charges. This phenomenon is called dipole radiation, motion of these charges will result in radiation of light with its maximum intensity in a plane normal to the direction of vibration of the charges and this radiation (light) will be polarized along the direction of vibration. The direction of vibration of the electric vector of the scattered radiation is at right angle to the scattering plane, the plane containing the incident and scattered rays. We can determine the scattering mechanism by the measurement of linear polarization.

To illustrate above phenomenon, we consider a thin cloud of small isotropically distributed spherical particles or dust grains. When a beam of unpolarized light passes through the cloud along Z-axis due to the transverse nature of the light the particle or molecule of the cloud start oscillating in x-y plane as shown in **figure 4.2.**

We can write the equation of motion of any of the charge or molecule as

$$x(t) = A\cos\phi\ e^{i\omega t}$$

$$y(t) = A\sin\phi\ e^{i\omega t}$$

$$z(t) = \text{Constant} \qquad \text{---------- (4.2)}$$

Differentiating Eq^{n} (4.2) twice, substituting in Eq^{n}(2.5) and deriving the Stoke's vector, according to Eq^{n} (2.6), we get

$$S = \left(\frac{qA}{c^2 R}\right)^2 \omega^4 \begin{bmatrix} \sin^2\phi + \cos^2\phi\cos^2\theta \\ \sin^2\phi - \cos^2\phi\cos^2\theta \\ 2\sin\phi\cos\phi\cos\theta \\ 0 \end{bmatrix} \qquad \text{----------(4.3)}$$

where the ϕ is the angle between the x-axis and the direction of the oscillation of the charge. From above equation we can say that the scattered beam polarization depends upon the azimuth angle ϕ and the position angle of the observer θ.

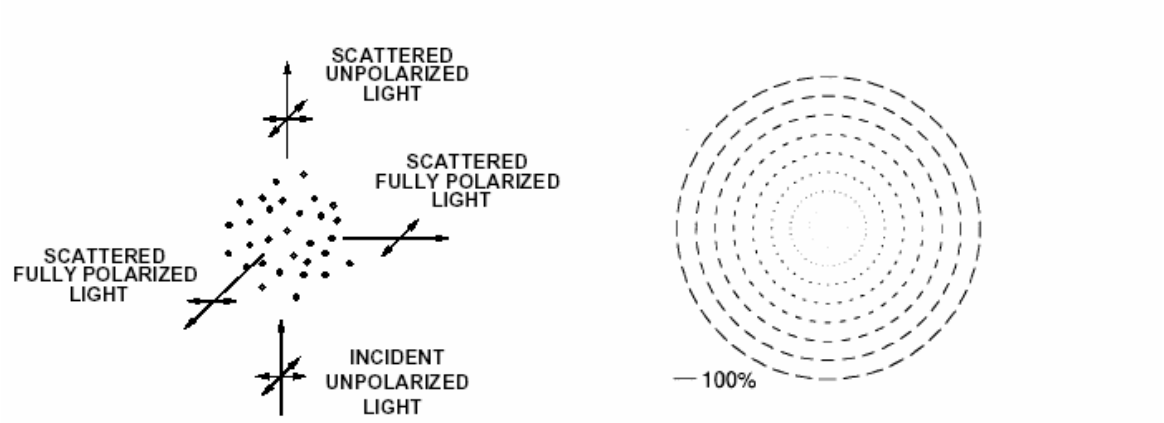

Figure (4.3): Polarized radiation due to scattering geometry

To understand this phenomenon how the center of scattering medium (dust or molecule cloud) as whole affects the polarization property of light passing through it. (Figure 4.3) we will consider Stokes vector of a beam which is made by combining many independent beams is the just the sum of the Stoke's vector of the components. Thus the polarization state of the radiation scattered by the ensemble of scattering centers is obtained by the integrating each of the Stoke's

parameter in Eq^{n} (4.3). Over all values of ϕ between 0 and 2π **(Ramaprakash 1998).**Thus for entire cloud

$$S_{cloud} = \pi\left(\frac{qA}{c^2 R}\right)^2 \omega^4 \begin{bmatrix} 1+\cos^2\theta \\ 1-\cos^2\theta \\ 0 \\ 0 \end{bmatrix} \qquad \text{----------(4.4)}$$

this radiation is always linearly polarized except for $\theta = 0^o$ and $\theta = 180^o$ in this case it becomes unpolarized. The radiation will be fully polarized for $\theta = 90^o$.

The degree of polarization is given by

$$\Pi = \frac{1-\cos^2\theta}{1+\cos^2\theta} \qquad \text{----------(4.5)}$$

4.4 Interstellar polarization

Interstellar (IS) polarization arises from the scattering of non-spherical dust grains that are aligned by the galactic magnetic fields, or molecular clouds that are present in between the source and observer. IS polarization is wavelength dependent and empirically expressed as

$$p_\lambda = p_{\max} e^{-k \ln^2(\lambda_{\max}/\lambda)} \qquad \text{----------(4.6)}$$

p_{max} ~ maximum polarization

λ_{max} ~ wavelength at which polarization is maximum

k ~ width of Serkowisky relation

5. T Tauri star

5.1 Introduction of T Tauri star

T Tauri stars (TTS) are newly born, roughly solar mass stars that have only recently emerged from their parent molecular cloud cores to become optically visible. T Tauri star are mostly found in active star formation regions. TTS are also known as irregular variable star, with amplitude typically of 1 or 2 magnitude, but which can occasionally reach magnitude 5. The time scale of these variations varies from a few minutes to hundreds of days **(P.Bastine)** .T Tauri stars are generally of two types:

1- **Classical type T Tauri (CTTS)**

2- **Weak type T Tauri star (WTTS)**

Classical TTS (CTTS) are surrounded by active accretion disks, and directly or indirectly, most of the excess emission seen in these stars can be attributed to the presence of the disk. The size of T Tauri disk could be near about 100 AU in radius and might even outshine the central star in their early stages **(Lynden-Bell & Pringle et al 1974).**

WTTS are also newborn stars like as CTTS but they do not have accretion disk. Then photometric variation and excess emission are powered by the cool spots and magnetic energy dissipation **(Hartmann, 1998).**

5.2. Polarization mechanism in T Tauri star

The polarization in T Tauri stars usually arises due to scattering from circumstellar disk, which lie outside the high temperature gaseous region **(Bastien 1982)** but it may also arise because of scattering by molecules, atoms, and electrons in stellar photosphere. One way to identify photosphere polarization is to detect change in the linear polarization across absorption or emission features, which are produced in the atmosphere of the star. Stellar light that is scattered off circumstellar **(CS)** dust grains will result in the light being polarized. But in the case of spherically symmetric shells, or face-on circular disks, no net polarization will be observed as all polarization vectors cancel out each other. On the other hand, in the cases of a deviation from the circular symmetry on the sky, a net polarization will be observed **(Oudmaijer 2001)**.

5.3. The complex photometric & polarimetric Behavior

The main problem with studying and understanding the variability of T Tauri stars is the range and complexity of their behavior. They can vary on time scale of minutes to years **(Herbst 1986)** & variation can have different characteristics at different wavelengths **(Herbst, Holtzman and Phelps 1982)**. Probably the luminosity variation in T Tauri stars is due to both variation in the gas emission region close to the star and variable obscuration by circumstellar material. But in some cases, the variation is due to only one of these processes.

5.4. UXOR Phenomena

Fig (5.1) Dust clump is not in our line of sight

Fig (5.2) Dust clump is in our line of sight

So for established facts explain that of the T Tauri stars show increased polarization when the optical light of the star is faint & redder at fainter magnitude, while in extreme visual minima there is a color reversal, this phenomena is known as **Ux Ori (UXOR)** phenomenon. To understand this phenomenon some scientists have suggested that this is due to the existence of dust clumps located in a disk like configuration rotating around the star (Figure 5.2). When the dust clumps are not in our line of sight (Figure 5.1), the star will be observed at maximum light, with only a slight contribution of scattered radiation from the dust. If the dust clump is intersecting the line of sight, light from the star will be absorbed, and the relative contribution of scattered light increases, increasing the observed polarization.

Moreover, the fact that the reddening of the star coincides with the reduction in brightness leaves little doubt that dust absorption indeed plays the main role in the process. In the case of extremely deep minima, the light from the star is blocked almost entirely, resulting in a “blueing “ of the energy distribution,

as now mostly scattered light dominates the observed light. Depending on the distribution of dust-clouds, the light can be more or less absorbed during a period of photo-polarimetric monitoring. Added complications to this simplified scenario are aligned grains and dust production and destruction. **(Oudmauijer 2001)**.

If the intrinsic polarization of T Tauri star originates from the optical dichroism of CS non-spherical grains then for a fixed wave length λ the degree of intrinsic polarization (P_{in}) related to optical thickness of the dust cloud which is crossing the line of site is given by

$$p_{in} = \frac{e^{-\tau_\perp} - e^{\tau_\parallel}}{e^{-\tau_\perp} + e^{\tau_\parallel}} \qquad \text{--------(5.1)}$$

Where $\tau_\perp$ and $\tau_{||}$ are the dust cloud optical thickness at wavelength λ for radiation with electric vector being perpendicular and parallel to the direction of the grains aligning correspondingly **(Grinin 1995)**. If $\tau_\perp - \tau_\parallel << 1$ then $\tau = \tau_\parallel$ we can rewrite the Eq^n(5.1)

$$P_{in} \approx \frac{\tau}{2}(1-\alpha) \qquad \text{-------- (5.2)}$$

Where $\alpha = \tau_\perp / \tau_\parallel$ is the factor to specify the non-spherical particles aligned in dust cloud.

On the other hand, when star is eclipsed by the dust clump, the photometric magnitude change is given by the:

$$\Delta m = -2.5 \log e^{-\tau} \qquad \text{------(5.3)}$$

From Eq^n (5.2) & (5.3) we get a relation between brightness variation and polarization degree.

$$P_{in} = a\Delta m \qquad \text{-----(5.4)}$$

Where a is the factor, which depends upon the degree of alignment of dust particle in the cloud.

But if the intrinsic polarization was produced due to the scattering of stellar radiation in the CS dust envelope then the dependence of intrinsic polarization degree and change in stellar brightness is quite different. In this case polarized

radiation arises due to the scattering of stellar radiation in circumstellar dust envelope. Here we assumed that direct stellar radiation in unpolarized. Therefore, when star is eclipsed by the dust cloud, the polarization degree of total radiation has to be increased in accordance with the decreasing of total radiation flux of "Star + Scattering envelope "system **(Grinin 1995)**:

$$P_{in}(\Delta m) = P_{in}(0)10^{0.4\Delta m} \qquad \text{------- (5.5)}$$

Here $P_{in}(0)$ is the polarization at bright state (when brightness is maximum).But in real situation, the relation between P_{in} and Δm will be somewhat different since the observed polarization is always a sum of the intrinsic and interstellar polarization.

$$\mathbf{P_{obs}\,(\Delta m) = P_{is} + P_{in}(\Delta m)}$$

6. Calculation of polarization

The polarization characteristics of any optical component can be conventionally expressed in terms of a Mueller matrix. Stokes vector **S** of light incident on the component defined by Mueller matrix M and the Stokes vector **S'** of the light emerging from the component are related

$$\mathbf{S' = M.\ S} \qquad \text{-------- (6.1)}$$

The Mueller matrix for a half wave plate with its optic axis at a position angle α is given by

$$M_H = \begin{bmatrix} 1 & 0 & 0 & 0 \\ 0 & \cos 4\alpha & \sin 4\alpha & 0 \\ 0 & \sin 4\alpha & -\cos 4\alpha & 0 \\ 0 & 0 & 0 & -1 \end{bmatrix} \qquad \text{------- (6.2)}$$

and that of an ideal analyzer with its axis at an angle θ

$$M_P = \frac{1}{2}\begin{bmatrix} 1 & \cos 2\theta & \sin 2\theta & 0 \\ \cos 2\theta & \cos^2 2\theta & \frac{1}{2}\sin 4\theta & 0 \\ \sin 2\theta & \frac{1}{2}\sin 4\theta & \sin^2 2\theta & 0 \\ 0 & 0 & 0 & 0 \end{bmatrix} \qquad \text{--------(6.3)}$$

Therefore, the Mueller matrices corresponding to ordinary (I_o) and extra ordinary rays (I_e) emerging from the Wollaston prism are obtained by $\theta = 0^o$ and $\theta = 90^o$ in Eq^n (6.3). On combining these Eq^n (6.1), Eq^n (6.2), the Stokes vector of the light emerging from the half wave plate (HWP) is obtained in terms of that of incident light, as

$$\begin{bmatrix} 1 & 0 & 0 & 0 \\ 0 & \cos 4 & \sin 4\alpha & 0 \\ 0 & \sin 4\alpha & -\cos 4\alpha & 0 \\ 0 & 0 & 0 & -1 \end{bmatrix} \cdot \begin{bmatrix} I \\ Q \\ U \\ V \end{bmatrix} = \begin{bmatrix} I \\ Q\cos 4\alpha + U \sin 4\alpha \\ Q\cos 4\alpha - U \sin 4\alpha \\ -V \end{bmatrix} \qquad \text{--------- (6.4)}$$

The orthogonal polarization components produced by the Wollaston prism analyzer are given by

$$\frac{1}{2}\begin{bmatrix} 1 & \pm 1 & 0 & 0 \\ \pm 1 & 1 & 0 & 0 \\ 0 & 0 & 0 & 0 \\ 0 & 0 & 0 & 0 \end{bmatrix}\cdot\begin{bmatrix} I \\ Q\cos 4\alpha + U\sin 4\alpha \\ Q\cos 4\alpha - U\sin 4\alpha \\ -V \end{bmatrix} = \frac{1}{2}\left[I \pm Q\cos 4\alpha \pm U\sin 4\alpha\right]\begin{bmatrix} 1 \\ \pm 1 \\ 0 \\ 0 \end{bmatrix} \quad \text{----- (6.5)}$$

where the + signs are for the polarization component at θ = 0° (I_o) and the – signs are for the one at θ = 90° (I_e).The ratio R(α)is obtained as

$$R(\alpha) = \frac{I_o - I_e}{I_o + I_e} = \frac{Q\cos 4\alpha + U\sin 4\alpha}{I} \quad \text{---------(6.6)}$$

$$= q\cos 4\alpha + u\sin 4\alpha$$

From Eq^n(2.3),we get

$$q = p\cos 2\theta \quad \text{And} \quad u = p\sin 2\theta \quad \text{----------(6.7)}$$

on substituting in Eq^n(6.4),we get

$$R(\alpha) = p\cos(2\theta - 4\alpha), \quad \text{----------(6.8)}$$

Here the normalized stokes parameter q & u are the ratio $R(\alpha)$ of the difference between the intensities of the ordinary and extraordinary rays to their sum at two different position of the half wave plate.

$$q = \frac{I_o(0^o) - I_e(0^o)}{I_o(0^o) + I_e(0^o)} \text{ and } \quad u = \frac{I_o(22.5^o) - I_e(22.5^o)}{I_o(22.5^o) + I_e(22.5^o)}$$

where $p = \sqrt{q^2 + u^2}$ and $\theta = \frac{1}{2}\tan^{-1}\left(\frac{u}{q}\right)$ --------(6.9)

Where p and θ are the degree of polarization and position angle of the object respectively.

*** This calculation of polarization is based on IMPOL.**

(A.N.Ramaprakash 1998)

6.1 Flat field errors

As we know that observations at atlest two positions of the half wave plate are required to determine the total intensity, degree of polarization and position angle of the object. But the situation is not that simple because the responsivity of the system is not same for the two orthogonal components of linear polarized light and

the responsivity of the CCD is a function of the position of the surface. Due to this effect we measure the signal, which is given by

$$I_e^{'}(\alpha) = I_e(\alpha)F_e \qquad \text{and} \qquad I_o^{'}(\alpha) = I_o(\alpha)F_o \qquad \text{-------(6.10)}$$

where $I_e(\alpha)$ and $I_o(\alpha)$ are the flux values in the images and F_e and F_o represent the effect mentioned above. The F_e and F_o don't change during the observation for a object so we can write the ratio of the F_o / F_e as

$$\frac{F_o}{F_e} = \left[\frac{I_o^{'}(0^o)}{I_e^{'}(45^o)} \times \frac{I_o^{'}(45^o)}{I_e^{'}(0^o)} \times \frac{I_o^{'}(22.5^o)}{I_e^{'}(67.5^o)} \times \frac{I_o^{'}(67.5^o)}{I_e^{'}(22.5^o)} \right]^{1/4} \qquad \text{-------(6.11)}$$

now the actual ratio of the fluxes in the two images can be written as

$$\frac{I_e}{I_o} = \frac{F_o}{F_e} \times \frac{I_e^{'}(\alpha)}{I_o^{'}(\alpha)} \qquad \text{----------(6.12)}$$

6.2 Error calculation due to photon noise

The error in polarization due to the photon noise can be theoretically calculated. If the number of photoelectron collected in ordinary and extraordinary images at any position of the half wave plate are respectively N_o and N_e , then the ratio $R(\alpha)$ is given by

$$R(\alpha) = \frac{N_o - N_e}{N_o + N_e} \qquad \text{----------(6.13)}$$

The error in determination of $R(\alpha)$, due to error associated with the determination of photoelectron count, is given by

$$(\Delta R)^2 = \left(\frac{\partial R}{\partial N_o} \right)^2 (\Delta N_o)^2 + \left(\frac{\partial R}{\partial N_e} \right)^2 (\Delta N_e)^2 \qquad \text{----------(6.14)}$$

If we assume that the determination of N_o and N_e are only affected by the photon noise then we get

$$(\Delta N_o)^2 = N_o + N_B \quad \text{and} \quad (\Delta N_e)^2 = N_e + N_B \qquad \text{--------- (6.15)}$$

where N_B is the background photoelectron counts. Substituting Eq^n (3.13) and Eq^n (3.15) into Eq^n (3.14), we get

$$(\Delta R)^2 = \frac{4N_o N_e}{(N_o + N_e)^3} + \frac{4N_B}{(N_o + N_e)^4}(N_o^2 + N_e^2) \qquad \text{----------(6.16)}$$

The error associated with p is given by

$$(\Delta p)^2 = \left(\frac{p}{q}\right)^2 (\Delta q)^2 + \left(\frac{u}{p}\right)^2 (\Delta u)^2 \qquad \text{---------(6.17)}$$

For small values of p, N_o and N_e are equal,and $N_b = 2\,N_B$, Eq^n (3.16) reduces to

$$(\Delta R)^2 = \frac{N + N_b}{N^2} \qquad \text{----------(6.18)}$$

we can see that, this expression is independent of the position angle of the half wave plate ,so

$$(\Delta q)^2 \sim (\Delta u)^2 \qquad \text{-----------(6.19)}$$

from this we get

$$(\Delta p)^2 = (\Delta R)^2 \text{ and } (\Delta\theta)^2 = \frac{1}{4}\left(\frac{\Delta p}{p}\right)^2 \quad) \qquad \text{----------(6.20)}$$

and for small polarization ,the error measurement of p and θ are given by

$$\sigma_p = \frac{\sqrt{N + N_b}}{N} \quad \text{and } \sigma_\theta = 0.5 \times \frac{\sigma_p}{p} rad \qquad \text{----------(6.21)}$$

7. Observations

7.1 Targets

We have selected 20 bright objects (T Tauri stars) for observation, in which 16 are highly photo-polarimetric variables they show variability of 1 to 4 magnitudes and few of them are periodic photo-polarimetric variables. They show polarization change of 0.4% to 15% with luminosity variation and four of them are suspected UXOR variables.

In the photometric observation, due to atmospheric effects we cannot observe below the 45^o from zenith. The longitude and latitude of **VBO** are respectively **78^o 50'** and **12^o34**' so we have added and subtracted 45^o into latitude to find the upper limit and lower limit of declination, so the declination (dec) range at Kavalur is -34.43^o to 57^o.

Due to cloudy weather at VBO in September we could not observe. But in January and February we got some clear nights and we observed four T Tauri stars Bf Ori, Ux Ori, Su Aur and Co ori in these observing runs. The R.A. and dec ranges for this observing runs are given in the table no 1.The calculation of the R.A. ranges is based on the formula given below

$$LST = H.A. + R.A$$

LST-Local sidereal time

H.A.- Hour Angle

R.A. – Right Ascension

S.No	Observing run	R.A. (hr)	Dec
1	14-09-04 to 19-09-04	15.2 to07.2	-34.43^o to 57^o
2	13 –01-05 to 18-01-05	23.3 to 15.5	-34.43^o to 57^o
3	08 –02-05 to 11-02-05	01.5 to 16.5	-34.43^o to 57^o

Table no.1 (Observing run and R.A. & Dec ranges)

The name, polarization change and luminosity change in V band, coordinates, magnitudes and rotation period of the targets are given in the **table no. 2**.These targets have taken from the **Bastien 1982**, **Astronomy Astrophysics Supplement Series 48,153-164 and Oudmaijer 2001,A&A 379 564-578, ESO**.

S.No.	Star name	P.C.(%)	P.V.(V)	Mag (v)	R.A.	Dec.	R.P.	Type
1	Bm And	6	12 to 14	12.40(B)	23 3738.48	+48 2413 12		V
2	Ww Vul	6	12 to 14	10.51	19 25 58.75	+21 12 31.3		V
3	Ak Sco	> 0.5		9.14	16 54 44.85	-36 53 18.6		V
4	Ry Lup	0.5 to 3		11.1	15 59 28.39	-40 21 51.2		V
5	Bf Ori	5	10 to 12	10.3	05 34 47.21	-06 35 00.6		V
6	Ry Ori	4	By 1	10.80(B)	05 32 09.92	-02 49 49.8		V
7	Hk ori	1 to 2	By 0.4	11.89	05 31 28.04	+12 09 10.3		V
8	Co ori			10.6	05 27 38.34	+11 25 38.9	2.7 or 1.6	V
9	Su Aur	0.4		9.42	04 55 59.38	+30 34 01.5	7.6	V
10	Hl Tau	15		14.56	04 31 38.4	+18 13 59	2.8	V
11	T Tau	1		9.60(B)	04 21 59.43	+19 32 06.4		V
12	Dk Tau	1 to 2	By 1	12.6	04 30 44.28	+26 01 24.6	5.6	V
13	Ry Tau	6	12 to14	10.21	04 21 57.41	+28 26 35.6		V
14	Bh cep	0.2 -2	By 1	10.8	22 01 42.87	+69 44 36.5		V
15	Ak Sco	> 0.5		9.14	16 54 44.85	-36 53 18.6		V
16	V350 Ori			10.4	05 40 11.9	-09 42 09		S.V
17	Nv Ori			9.5	05 35 31.25	-05 33 11.8		S.V
18	Cq Tau			10.7	05 35 58.47	+24 44 54.1		S.V
19	Ux Ori			9.7	05 04 29.99	-03 47 14.3		S.V
20	Xy Per			9.44	03 49 36.374	+38 58 55.5		S.V

Table No.2: List of the Targets (T Tauri Stars)

P.C. - Polarization change

P.V. - Photometric variation

V - UXOR variable

S.V. - Suspected UXOR variables

7.2 Finding Charts

When we point the telescope towards the target, we get an image on the CCD of sky of '3 arc min X 3 arc min'. We match this image to finding chart of the same star, if both images are looking alike then the direction of telescope is correct and it is pointing at right point. These finding charts were made from United States Naval Observatory (USNO) website **(**http://www.nofs.navy.mil/data**)**. The size of finding charts are '5 arc min X 5 arc min' and these R band images, which are taken from the digitized sky survey –2 (DSSR2).

7.3 Data collection

To understand the photo polarimetric variation & UXOR phenomenon of T Tauri stars. We made polarimetric observations to collect data for this studies using IMPOL by 2.3-meter telescope at **Vainu Bappu Observatory** during three observing runs between **September 2004 to February 2005**.

Due to cloudy weather and lack of time, Out of 20 targets, which we had selected for this study, only 4 objects were observed. Two standard polarized stars and one unpolarized star were also observed.

For each set of data we have taken four exposures at four different orientations (0,22.5,45 and 67.5) of half wave plate (HWP).

The exposure time should be selected such way that ordinary and extraordinary ray do not merge in each other. The aperture of images should be less then the grid width that is approximate 22 pixels so that images do not cut by the edges of the grid and we get sufficient counts to minimize the error, which is due to photon noise (See section 6.2). We have chosen the exposure time such that we got more than 5000 counts per pixel, which is sufficient for minimizing the error. The exposure time for each star is given in the table 1.

S.No	Star name	Exposure time (seconds)
1	HD19820	05
2	BD+64d106	20
3	Su Aur	05
4	Co Ori	60
5	Ux Ori	10
6	Bf Ori	20

Table 3:Star name and Exposure time

Two images are formed on the main CCD for each target; these two images correspond to the two orthogonal components ordinary and extraordinary respectively of linearly polarized light (Figure 8.1). The ratio (R) of the difference between the flux collected in to the two images to their sum, at different orientations (α) of the HWP, are related to the normalized Stokes parameter as

$$R(0^o) = -R(45^o) = q \quad \text{and} \quad R(22.5^o) = -R(67.5^o) = u$$

The degree of polarization p and position angle θ are related by the ratio *R* is given by

$$R(\alpha) = p\cos(2\theta - 4\alpha)$$

for details see chapter 6.

8. Data reduction

The data reduction of the FITS images, which we get from IMPOL CCD, has been done by the IRAF (Image Reduction and Analysis Facility) at IUCAA.IRAF is provided by the National Optical Astronomy Observatories. We have used phot task of apphot package to calculate fluxes of the ordinary and extraordinary rays of IRAF software.

Aperture photometry is the measurement of light, which falls inside a particular aperture; usually, we take a circular aperture of some fixed size. The technical term Full-Width Half-Maximum, or FWHM, is used to describe a measurement of the width of an object in an image, when that object does not have sharp edges. A simple box can be described just by its width, and a rectangle by its width and height. However, the image of a star in an astronomical image has a profile which is closer to a Gaussian curve phot task does aperture photometry on given star and calculate flux at given aperture phot task have several parameter like image, skyfile, coords, output, datapars, centerpars, fitskypars, photpars etc.

Image: In image parameter we give the name of fits file.

Coords: Coords parameter contains a text file of the list of the centers of the objects (stars) in that fits file. This coords file can be made manually or we can use daofind task. The extension of this file is "coo".

Output: Output parameter contains the name of the results file, which is received on running phot task. The extension of this file is "mag"

Datapars: Datapars parameter contains the name of the file containing the data dependent parameters like fwhmpsf and sigma.

Centerpars: Centerpars contain the name of the file containing the centering parameters. The critical parameters calgorithm and cbox are located here.

Fitskypars: The name of the text file containing the sky fitting parameters. The critical parameters salgorithm, annulus, and dannulus are located here.

Photpars: The name of the file containing the photometry parameters. The critical parameter apertures are located here.

Some critical parameter like full width at half maximum (FWHM) and sigma of datapars were determine by the imexamine task and few important plots

like radial profile plots, surface plot, histogram plot and contour plot of the image can also be seen by the this task.

FWHM can be computed using the enclosed flux radial profile. We can use one of the fit Gaussian or Moffat profile to the enclosed flux profile. The selected profile fit to the individual pixel values. We have used Gaussian fit for calculating FWHM. The FWHM of apertures used for photometry of the stars are listed in table no.4.

Star	FWHM	Aperture
HD19820	5.5	14
BD+64d106	5.5	14
Su Aur	4	09
Co Ori	5.6	14
Ux Ori	5.9	15
Bf Ori	5.8	14

Table no.4 (FWHM and Apertures)

The exact center of the star can be computed by the using different algorithms like none, centroid and gauss.

None: In this algorithm initially given positions of the centers are assumed to be correct values of the centers.

Centroid: This algorithm computes the intensity weighted means of the marginal profiles in x and y for determining the center of the object.

Gauss: The object centers are computed by fitting a Gaussian of fixed fwhmpsf, specified by the DATAPARS fwhmpsf parameter, to the marginal profiles in x and y using non-linear least squares techniques.

But out of these we used centroid algorithm for determining the center of the ordinary and extraordinary ray images.

Sky Calculation

Sky values determination is the most crucial part of this data reduction because the sky around the stars is dominated by photo noise (see chapter 6). The center of the ordinary and extra ordinary ray separated by only approximately 30 pixels. The aperture of the stars is near about 12 pixels for most of the stars, so we cannot take an annulus around stars because the annulus picks light from other star (Ordinary or Extra ordinary ray image).

Sky values of background can be determined by taking an annulus of width of 5 to 10 pixels, using any algorithm from mean, median, mode, centroid, gauss and crosscor. We only use this method for one star namely Su Aur because the aperture of this star is quite less, it is about 9 pixels. We used crosscor algorithm for calculation of sky values in Su Aur by taking an annulus width of 5 pixels.

Crosscor algorithm calculates the sky values by using the cross-correlation function of the sky pixel histogram and a Gaussian noise function with a sigma equal to the computed sigma of the sky pixel distribution.

We used constant algorithm for other stars. The value of background sky for other three T Tauri stars and two Standard polarized star have been calculated by taking a box of 12 X 20 pixels above the stars (ordinary and extraordinary ray) from the imexamine or imstat task. These both tasks can give mean and median values of the sky with in box. We used median values of sky as a sky value of the star. The sigma (standard deviation) of the values of sky pixel with in the box is approximately 6.

Aperture for photometry: Aperture should be taken such a way that the noise from the background is minimized and signal from object is maximum. If we draw a graph between the radius of the aperture and the total number of the count of the object within the aperture, it will grow initially, but start flattening after some radius. So we can chose this radius as an aperture radius or a good estimation of the aperture for a bright star is 2.5 times of its FWHM value and we have followed this estimation in our calculations.

A program in C is written, which computes the polarization at each aperture (See Appendix).

One of the data file CO10.fits is shown in figure (8.1). This is an image of Co Ori at the 0 position of the HWP. In this field (image) two stars can be identified in the center appearing as stars which in fact are the two orthogonal polarized components parallel & perpendicular to the axis of the Wollaston prism, called ordinary (I_o) and extraordinary image (I_e) of the Co Ori. This image has taken in R band by IMPOL on 08 February 05 at VBT. You can also see a pattern or set of vertical columns. This is an image of grid. The value of a single Stokes parameter (q or u) can be determined from one such image.

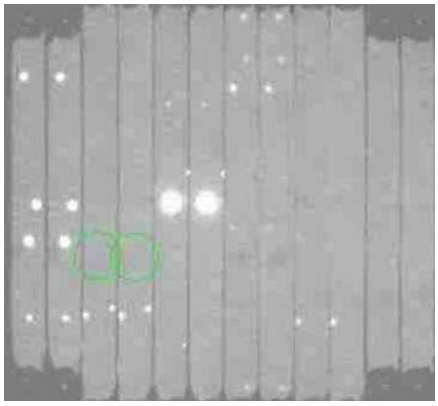

Figure 8.1 (CCD image of Co Ori)

9. Results and Conclusion

Simultaneous photo-polarimetric measurements in R band have been made, on four classical T Tauri stars. But due to lack of data, simultaneous photo-polarimetric variation could not be shown, but polarization in four stars were observed and two standard polarized stars were observed for calibrating the instrument. The results are shown in table no.5. This table contains the name of stars, name of the images, degree of polarization and position angles, previously published values of polarization and position angles, and error in the current calculation of degree of polarization and position angle. The first column of the table contains the name of stars. In the second column the names of the images are given the first number in image name correspond to the set number and the two numbers after the underscore like 01 or 23 correspond the HWP. The 0,1,2, and 3 correspond to the position of HWP at the angle of 0,22.5,45 and 67.5 degree respectively. From the 0 and 1 position of HWP we get the normalized Stokes parameter q and u respectively and from 2 and 3 we get –q and -u (See chapter 6). The image name Aur2_23 corresponds to second set of the data at HWP positions 45 and 67.5 respectively. Third column contains the observed values of the degree of polarization based on the Eq^{n} (6.9). Next column contain the values of the degree of polarization, which is previously published by some one. These stars have variable degree of polarization so in some cases I have given the range of the variation of the polarization. The fifth column contains the error (σ_p) in the calculation of the degree of polarization. This has been calculated by the Eq^{n} (6.21). We have not subtracted instrumental polarization from observed polarization because instrumental polarization is not coming constant.

The next column contain values of observed position angles based on this Eq^{n}(6.9)

$$\theta = \frac{1}{2}\tan^{-1}\left(\frac{u}{q}\right)$$

To calculate the position angle we have taken universally accepted convention that the position angle as referred to the celestial north-south pole axis passing through the point in the sky where the observation is made –0° is towards north and 90° towards east. The position angle is quoted in the range $0^o < \theta < 180^o$.

The convention for calculating position angles is

$\theta_{cal} = \frac{1}{2}\tan^{-1}\left(\frac{\lvert R(22.5^0)\rvert}{\lvert R(0^o)\rvert}\right)$			$\theta_{cal} = \frac{1}{2}\tan^{-1}\left(\frac{\lvert R(67..5^0)\rvert}{\lvert R(45^o)\rvert}\right)$		
R (0°)	**R (22.5°)**	θ	**R (45°)**	**R (67.5°)**	θ
+	-	θ_{cal}	-	+	θ_{cal}
-	-	$90-\theta_{cal}$	+	+	$90-\theta_{cal}$
-	+	$90+\theta_{cal}$	+	-	$90+\theta_{cal}$
+	+	$180^o-\theta_{cal}$	-	-	$180^o-\theta_{cal}$

The next two columns contain the published values and the error in the calculation σ_θ in radians. This calculation is based on Eq^n(6.21).

The last column contains the total flux of the star I= I(e)+I(O) here I(e) and I(O) are the fluxes of extraordinary and ordinary image respectively**.**

From the one image we calculate the value of one Stokes parameter.

Star Name	Image name	Pol (%)	Pub (Pol)	σ_p	P.A. (deg)	Pub (P.A.) (deg)	σ_θ	I(e)+I(O)
Su Aur	Aur1_01	0.907	0.11	0.15	109.6	116	4.6	488541.6
Su Aur	Aur1_23	0.899	0.11	0.15	109.6	116	4.7	476194.2
Su Aur	Aur2_01	1.085	0.11	0.15	105.2	116	3.9	471422.5
Su Aur	Aur2_23	0.896	0.11"	0.15	103.6	116	4.8	465899.7
Bf Ori	Bf1_01	1.673	0.6	0.15	87.27	40 - 80	2.5	485204.5
Bf Ori	Bf1_23	1.616	0.6	0.15	86.03	40 - 80	2.6	481938.6
Bf Ori	Bf2_01	1.447	0.6	0.15	93.3	40 - 80	2.9	467606.1
Bf Ori	Bf2_23	1.456	0.6	0.15	86.54	40 - 80	3	450728.6
Bf Ori	Bf4_01	1.656	0.6	0.15	91.93	40 - 80	2.7	437055.5
Bf Ori	Bf4_23	1.257	0.6	0.15	82.45	40 - 80	3.5	439326.6
Co Ori	Co1_01	1.682	1.6 - 2.6	0.11	163.1	155 -170	1.9	799723.3
Co Ori	Co1_23	1.651	1.6 - 2.6	0.11	159	155 -170	2	798797.9
Co Ori	Co2_01	1.696	1.6 - 2.6	0.12	151.9	155 -170	2	749110.6
Co Ori	Co2_23	1.669	1.6 - 2.6	0.12	155	155 -170	2	736873.1
Co Ori	Co3_01	1.998	1.6 - 2.6	0.12	159	155 -170	1.7	741793.1
Co Ori	Co3_23	2.028	1.6 - 2.6	0.12	160	155 -170	1.7	725298.7
Ux Ori	Ux1_01	1.422	0.8 -1.4	0.21	60.24	90 -110	4.2	249392.3
Ux Ori	Ux1_23	1.42	0.8 -1.4	0.21	73.1	90 -110	4.1	251934.5
Ux Ori	Ux2_01	1.429	0.8 –1.4	0.23	89.48	90 -110	4.7	199878.69
Ux Ori	Ux2_23	1.838	0.8 –1.4	0.21	62.49	90 -110	3.2	251309.6
Ux Ori	Ux3_01	1.871	0.8 -1.4	0.2	55.83	90 -110	3.1	257018.6
Ux Ori	Ux3_23	1.72	0.8 –1.4	0.21	65.88	90 -110	3.4	250775.2
Ux Ori	Ux4_01	1.428	0.8 –1.4	0.2	67.69	90 -110	4.1	255411
Ux Ori	Ux4_23	1.432	0.8 -1.4	0.21	65.43	90 -110	4.1	251350.8
Ux Ori	Ux5_01	1.617	0.8 -1.4	0.22	68.92	90 -110	3.9	223504.8
Ux Ori	Ux5_23	1.619	0.8 -1.4	0.2	65.46	90 -110	3.6	256145
Hd19820	HD1_01	4.888	4.5	0.09	116.4	114	0.5	1351187
Hd19820	HD1_23	4.756	4.5	0.09	116.5	114	0.5	1355271.2
Hd19820	HD2_01	4.747	4.5	0.09	118.3	114	0.5	1355850.4
Hd19820	HD2_23	4.794	4.5	0.09	118.2	114	0.5	1364984.2
Hd19820	HD3_01	4.813	4.5	0.09	117.9	114	0.5	1361270.2
Hd19820	HD3_23	4.879	4.5	0.09	117.9	114	0.5	1352478.7
BD+64d106	BD1_01	5.7	5.2	0.15	101.8	98	0.8	506264.3
BD+64d106	BD1_23	5.59	5.2	0.15	101.5	98	0.8	548087.5
BD+64d106	BD2_01	5.5	5.2	0.15	100.8	98	0.8	523445.5
BD+64d106	BD2_23	5.7	5.2	0.15	101.3	98	0.7	524572.6

BD+64d106	BD3_01	5.8	5.2	0.15	101.2	98	0.7	528688.9
BD+64d106	BD3_23	5.52	5.2	0.15	100.6	98	0.8	534824

Conclusion

Simultaneous photo-polarimetric observations in R band have been done, on four classical T Tauri stars. But due to lack of data, simultaneous photo-polarimetric variation could not be shown, but polarization in four stars were observed and two standard polarized stars were observed for calibrating the instrument. In order to estimate the linear polarization **p** and position angle θ, we have plotted our all data points R(α) with HWP angle (orientations) **α** . By using of χ^2 fitting technique we fitted a cosine curve to the Eq^n **$R(\alpha)=p\cos(2\theta-4\alpha)$** , (see figures).We have not eliminated instrumental polarization which is 0.3% in the R band for our data. The results are shown in table 6.Table 6 contains name, the degree of polarization of star, position angle and error.

Name	P(%)	σ_p	θ(Deg)	σ_θ (Deg)
Su Aur	0.09443	±0.0486	107.23	±1.47
Bf Ori	1.5	±0.0814	89.48	±1.55
Co Ori	1.77	±0.0898	155.82	±1.45
Ux Ori	1.52	±0.1130	64.05	±2.14

Table No. 6

Co Ori:

Oudmaijer (2001) found a gradual decrease in brightness over five days in October 1998 but very slight change in degree of polarization, from 2.4 to 2.6 % in I band. We also found degree of linear polarization 1.77 % in R band.

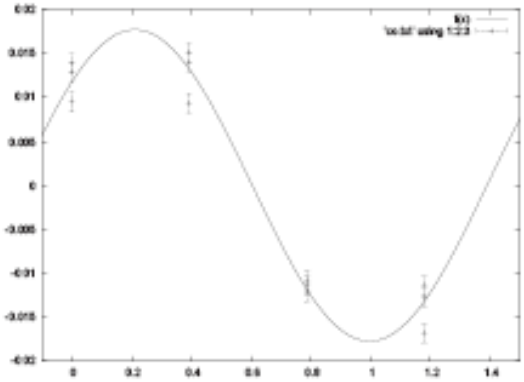

Figure 3: Co Ori

Ux Ori:

Ux Ori is the suspected UXOR variable and we found the degree of linear polarization 1.52% in our data in R band.

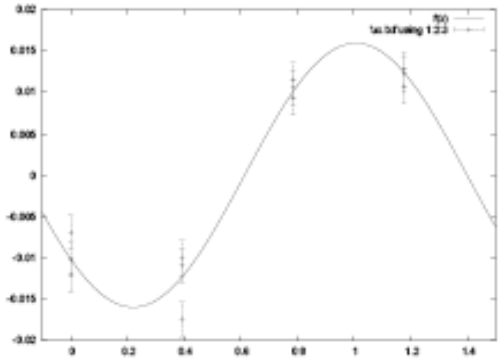

Figure 4: Ux Ori

BF Ori:

Due to lack of data we are not able to show any simultaneous photopolarimetric variation in BF Ori but the UXOR behavior was previously discussed by Grinin et al.(1989) for BF Ori. They have shown that at the time of minimum flux, polarization reaches to 5 %. We found the degree of linear polarization of BF Ori is near about 1.5 % .So from this data we can clearly say that at the time of observation the dust clump was not in our line of sight and this polarization is originated from the disk like configuration around the BF Ori.

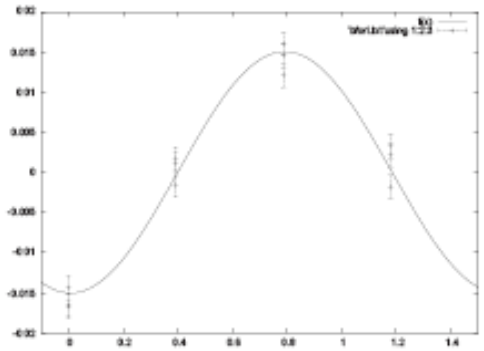

Figure 1: Bf Ori

Su Aur:

We could not find any simultaneous photo polarimetric variation in Su Aur from our data. We found 0.94% of degree of linear polarization in R band. Which conforms that the star has disk like configuration.

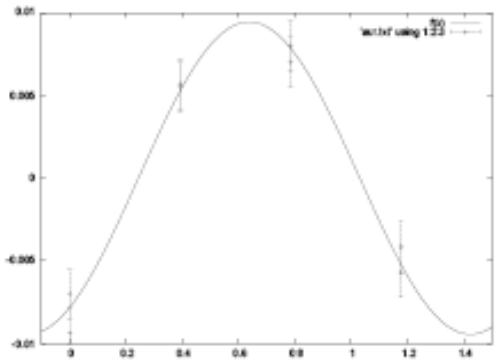

Figure 2: Su Aur

Appendix

This c program reads the output (*.mag) file which is received after running phot task and calculates the polarization and error at each aperture up to 20, according to the FWHM and radial profile plot we estimate the aperture of star and take the value of degree of polarization correspondingly and error correspondingly.

1) First part of the programme read oray and eray values from a file for each apperture value from 1 to 25.
2) Then its calculate the Flat fielding correction factor (f) for each of the apperture.
3) Then its calculate the polarization value q and u for each apperture.
4) Polarization value is calculated after sqaring and adding q and u value.
5) Final polarization value is the square root of this added value.

----------Code----------

```
#include<stdio.h>
#include<math.h>
struct star
{
  float oray[20];
  float eray[20];
};
struct star position[4];

struct sum
{
  float oray[20];
  float eray[20];
};
struct sum plate[4];
```

```
main()
{
 FILE *fp,*a;
 float  add[4][20],diff[4][20],ratio[4][20],pol[2][20];
 float factor[20],polp[2][20],polq[2][20],addray[20],addsum[20],error[20];
 int i,j,k;
 fp=fopen("hdset4.out","r");
 a=fopen("hdset4sum.out","r");
 if(fp==NULL)
      {
        printf(" input file does not exist");
         exit(0);
      }
 /*-------------------------------------------------------------*/
 for(j=0;j<20;j++)
   {
    factor[j]=1;
   }
        /*-----------------------------------------------------------*/
        for(i=0;i<4;i++)
        {
     for(j=0;j<20;j++)
         {
           fscanf(fp,"%f ",&position[i].oray[j]);
           printf("%f ",position[i].oray[j]);
         }
        printf("\n\n");
     for(j=0;j<20;j++)
         {
           fscanf(fp,"%f ",&position[i].eray[j]);
           printf("%f ",position[i].eray[j]);
         }
     printf("\n\n");
```

```
   }
   /*-------------------------------------------------------------*/
          for(i=0;i<4;i++)
   {
for(j=0;j<20;j++)
    {
      fscanf(a,"%f ",&plate[i].oray[j]);
      printf("%f ",plate[i].oray[j]);
    }
   printf("\n\n");
for(j=0;j<20;j++)
    {
      fscanf(a,"%f ",&plate[i].eray[j]);
      printf("%f ",plate[i].eray[j]);
    }
printf("\n\n");
   }

/*-------------------------------------------------------------*/
           for(j=0;j<20;j++)

    {
          for(i=0;i<4;i++)
   {
     factor[j]=position[i].eray[j]/position[i].oray[j]*factor[j] ;

    }
          factor[j]=pow(factor[j],.20);
          /*      printf("%f\n",factor[j]);*/
   }

/*-------------------------------------------------------------*/
   for(i=0;i<2;i++)
```

```
        {
      for(j=0;j<20;j++)
         {
           polp[i][j]=((position[i].oray[j]/position[i].eray[j])*factor[j]-
1.0)/((position[i].oray[j]/position[i].eray[j])*factor[j]+1.0);
         polq[i][j]=((position[i+1].oray[j]/position[i+1].eray[j])*factor[j]-
1.0)/((position[i+1].oray[j]/position[i+1].eray[j])*factor[j]+1.0);
        pol[i][j]=sqrt( polp[i][j]*polp[i][j]+polq[i][j]*polq[i][j]);

         addray[j]=position[i+1].oray[j]+position[i+1].eray[j];
         addsum[j]=plate[i+1].oray[j]+plate[i+1].eray[j];
         error[j]=sqrt(addsum[j])/addray[j];
         printf("%d  %d  %f   %f\n",i,j,pol[i][j],error[j]);
         }

        }
}
```

References

[1] A.N.Ramaprakash 1998, PhD thesis (IUCAA, Pune)

[2] V.P.Grinin, E.A.Kolotilov, A.Rosopchina, 1995;Astronomy Astrophysics Supplement Series 112,457-473

[3] Lee Hartmann, 1998,Accretion processes in star formation, Cambridge university press.

[4] Herbst 1986,Publication of the Astronomical Society of The Pacific

[5] Bastien 1982, Astronomy Astrophysics Supplement Series 48,153-164

[6] Bastien, Polarization in circum stellar System

[7] Lynden-Bell & Pringle 1974,M.N.R.A.S, 168,603

[8] Oudmaijer 2001,A&A 379 564-578, ESO

[9] Feynman 1998, The Feynman Lecture on Physics vol. 1, second edition, Narosa

[10] Hovenier J.W., 1994, Applied Optics 33, 8318

[11] H.C. van de Hulst1981, light Scattering by small particles, Drver Publication New Yark

[12] J.D.Jackson 1986,Classical elictrodynamics, second edition,Cambridge university press

[13] M.S.Longair[1] 1992,High-energy Astrophysics vol 1, Cambridge university press

[14] M.S.Longair[2] 1992,High-energy Astrophysics vol 2, Cambridge university press

[15] Pavan Chakraborty 2002,Phd thesis on cemetery dust (IIA, Bangalore)

[16] Serge Huard 1997,Polarization of light, John willy & sons publication.

[17] Tinbergen J., 1996, Astronomical Polarimetry, second edition,Cambridge

[18] http://www.nofs.navy.mil/data